Affine Invariant Geometry for Non-rigid Shapes

International Journal of Computer Vision manuscript No.
(will be inserted by the editor)

Affine invariant geometry for non-rigid shapes

Dan Raviv · Ron Kimmel

Received: date / Accepted: date

Abstract Shape recognition deals with the study geometric structures. Modern surface processing methods can cope with non-rigidity - by measuring the lack of isometry, deal with similarity or scaling - by multiplying the Euclidean arc-length by the Gaussian curvature, and manage equi-affine transformations - by resorting to the special affine arc-length definition in classical equi-affine differential geometry. Here, we propose a computational framework that is invariant to the full affine group of transformations (similarity and equi-affine). Thus, by construction, it can handle non-rigid shapes. Technically, we add the similarity invariant property to an equi-affine invariant one and establish an affine invariant pseudo-metric. As an example, we show how diffusion geometry can encapsulate the proposed measure to provide robust signatures and other analysis tools for affine invariant surface matching and comparison.

1 Introduction

Differential invariants for planar shape matching and recognition were introduced to computer vision in the 80's [60] and studied in the early 90's [13,12,20,14,17,16], where global invariants were computed in a local manner to overcome numerical sensitivity of the differential forms. Scale space entered the game as a stabilizing mechanism, for example in [15], where locality was tuned by a scalar indicating how far one should depart from the point of interest. Along a different path, using a point matching oracle to reduce the number of derivatives, semi-differential signatures were proposed in [57,58,38,44,18]. Non-local signatures, which are more sensitive to occlusions, were shown to perform favorably in holistic paradigms [40,11,41,33]. At another end, image simplification through geometric invariant heat processes were introduced and experimented with during the late 90's, [54,2,31]. At the beginning of this century, scale space theories gave birth to the celebrated *scale invariant feature transform* (SIFT) [35] and the affine-scale invariant feature transform ASIFT [39], that are used to successfully locate repeatable informative (invariant) features in images.

Matching surfaces while accounting for deformations was performed with conformal mappings [34], embedding to finite dimensional Euclidean spaces [26] and infinite ones [5, 53], topological graphs [29,59], and exploiting the Gromov-Hausdorff distance [36,8,19]. Which is just a subset of the numerous methods used in this exploding field. Another example, relevant to this paper is diffusion geometry, introduced in [22] for manifold learning that was first applied for shape analysis in [9]. This geometry can be constructed from the eigen-strucutre of the Laplace-Beltrami operator. The same decomposition was recently used in [56,42,43, 9] to construct surface descriptors for shape retrieval and matching.

Some approaches in the field of shape matching, measure the discrepancy between surfaces and volumes by weighing the effort it takes to deform one geometric structure into another. Such geometric constructions can be used to define a Riemannian metric on the space of all possible shapes. These methods are popular, for example, in medical information analysis. They incorporate statistical priors [23], use spherical harmonics [30], exploit global symmetric deformations [51], and use smooth diffeomorphic mappings [4]. Statistics of curved domains can be utilized, for example, to overcome uncertainty, to evaluate different hypothesis, and compare between observations [27,45]. The metric proposed in this paper applies to the way a single shape is treated

darav@mit.edu, Media Lab., MIT, USA

ron@cs.technion.ac.il, Dept. of Computer Science,Technion, Israel

Address(es) of author(s) should be given

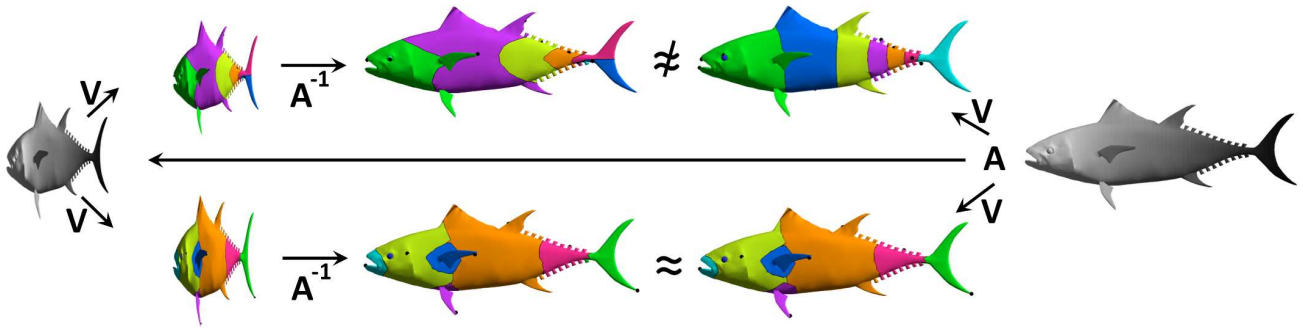

Fig. 1: Voronoi diagrams of ten points selected by farthest point sampling. Diffusion distances were used based on Euclidean metric (top) and an affine invariant one (bottom).

as a Riemannian structure rather than the space of all possible shapes as a whole.

In this paper, following the adoption of metric/differential geometry tools to image-analysis, we introduce a new geometry for affine invariant surface analysis. In [48,49], the equi-affine invariant metric was first introduced to the surface analysis arena. Invariant curvatures were studied in [52,3], and a scale invariant metric was the main theme of [1,10]. Here, we introduce a framework that handles affine transformations in its most general form including similarity. The proposed full affine invariant geometry for non-rigid surfaces copes with linear (affine) transformations including scaling and isometry.

The paper is organized as follows: In Section 2 we introduce the affine invariant pseudo-metric. Section 3 proves the invariance of the construction. In Section 4 numerical implementation considerations are discussed. Next, Section 5 briefly reviews some ideas behind diffusion geometry that could be used as a numerically stabilizing mechanism for the proposed geometry. Section 6 is dedicated to experimental results, and Section 7 concludes the paper.

2 Affine metric construction

We model a surface $(\mathcal{S}, g)$ as a compact two dimensional Riemannian manifold $\mathcal{S}$ with a metric tensor g. Let us further assume that $\mathcal{S}$ is embedded in $\mathbb{R}^3$ by a regular map $S : U \subset \mathbb{R}^2 \to \mathbb{R}^3$. The Euclidean metric tensor can be obtained from the re-parameterization invariant arc-length ds of a parametrized curve $C(s)$ on $\mathcal{S}$. As the simplest Euclidean invariant is length, we search for the parameterization s that would satisfy $|C_s| = 1$, or explicitly,

$$\begin{aligned} 1 &= \langle C_s, C_s \rangle = \langle S_s, S_s \rangle \\ &= \left\langle \frac{\partial S}{\partial u}\frac{du}{ds} + \frac{\partial S}{\partial v}\frac{dv}{ds}, \frac{\partial S}{\partial u}\frac{du}{ds} + \frac{\partial S}{\partial v}\frac{dv}{ds} \right\rangle \\ &= ds^{-2}\left(g_{11}du^2 + 2g_{12}dudv + g_{22}dv^2\right), \end{aligned} \tag{1}$$

where

$$g_{ij} = \langle S_i, S_j \rangle, \tag{2}$$

using the short hand notation $S_1 = \partial S/\partial u$, $S_2 = \partial S/\partial v$, where u and v are the coordinates of U. An infinitesimal displacement ds on the surface is thereby given by

$$ds^2 = g_{11}du^2 + 2g_{12}dudv + g_{22}dv^2. \tag{3}$$

The metric coefficients $\{g_{ij}\}$ translate the surface parametrization coordinates u and v into a Euclidean invariant distance measure on the surface. This distance would not change under Euclidean transformations of the surface $RS+\mathbf{b}$ where R is a rotation matrix in $\mathbb{R}^3$. It would also be preserved w.r.t. isometric (length preserving) transformations.

The equi-affine transformation, defined by the linear operator $AS+\mathbf{b}$, where $\det(A) = 1$, requires a different treatment, see [6,55]. Consider the curve $C \in \mathcal{S}$, parametrized by w. The equi-affine transformation is volume preserving, and thus, its invariant metric is constructed by restricting the volume defined by S_u, S_v, and C_{ww} to one. That is,

$$\begin{aligned} 1 &= \det(S_u, S_v, C_{ww}) \\ &= \det\left(S_u, S_v, S_{ww}\right) \\ &= \det\left(S_u, S_v, S_{uu}\frac{du^2}{dw^2} + 2S_{uv}\frac{du}{dw}\frac{dv}{dw} + \right. \\ &\qquad \left. S_{vv}\frac{dv^2}{dw^2} + S_u\frac{d^2u}{dw^2} + S_v\frac{d^2v}{dw^2}\right) \\ &= dw^{-2}\det\left(S_u, S_v, S_{uu}du^2 + 2S_{uv}dudv + S_{vv}dv^2\right) \\ &= dw^{-2}\left(r_{11}du^2 + 2r_{12}dudv + r_{22}dv^2\right), \end{aligned} \tag{4}$$

where now, the metric elements are given by

$$r_{ij} = \det\left(S_1, S_2, S_{ij}\right), \tag{5}$$

and we extended the short hand notation to second order derivatives by which $S_{11} = \frac{\partial^2 S}{\partial u^2}$, $S_{22} = \frac{\partial^2 S}{\partial v^2}$, and $S_{12} = \frac{\partial^2 S}{\partial u \partial v}$. Note, that the second fundamental form in the Euclidean case is given by $b_{ij} = \sqrt{g} r_{ij}$ where $g = \det(g_{ij}) = g_{11}g_{22} - g_{12}^2$. The equi-affine re-parametrization invariant metric [55,6] reads

$$q_{ij} = |r|^{-\frac{1}{4}} r_{ij}, \tag{6}$$

where $r = \det(r_{ij}) = r_{11}r_{22} - r_{12}^2$.

This equi-affine metric applies to surfaces with positive Euclidean Gaussian curvature, that are oriented so as to provide positive squared distances. See also [48]. At hyperbolic points, when the Euclidean Gaussian curvature is negative, we have one positive and one negative eigenvalue in the metric r. In this case, we set the metric tensor to be zero. Numerically, we assign $(q_{ij}) = \epsilon\mathcal{I} = \epsilon \begin{pmatrix} 1 & 0 \\ 0 & 1 \end{pmatrix}$ metric to that point, where ϵ is a small constant. That is, such regions would practically be ignored by the proposed geometry [50]. Note that as S is a compact manifold, we can define a continuous shrinkage of the metric while the error is kept at the order of ϵ. In our implementation we chose a small ϵ at all hyperbolic and parabolic points. It was numerically validated and supported by the experimental results for the non-trivial surfaces reported in this paper.

Next, we resort to the similarity (scale and isometry) invariant metric proposed in [1]. Scale invariance is obtained by multiplying the metric by the Gaussian curvature. In metric notations, the Gaussian curvature K is defined as the ratio between the determinants of the second and the first fundamental forms. We propose to compute the Gaussian curvature with respect to the equi-affine invariant metric, and then construct a new metric by multiplying the equi-affine metric elements by the equi-affine Gaussian curvature. Specifically, consider the surface $(\mathcal{S}, q)$, where q_{ij} is the equi-affine invariant pseudo-metric, and compute the equi-affine Gaussian curvature K^q of $(\mathcal{S}, q)$ at each point. The affine invariant pseudo-metric is then defined by

$$h_{ij} = |K^q|\, q_{ij}. \tag{7}$$

Let us next prove the affine invariance of the above construction for surfaces.

3 Invariance properties

In this section we prove affine invariance of the proposed pseudo-metric. Let us first justify the scale invariant metric constructed by multiplication of a given Euclidean metric by the Gaussian curvature.

Theorem 1 *Let K be the Gaussian curvature of a surface S, and g_{ij} the elements of its Riemannian metric. Then, $|K|g_{ij}$ is scale invariant metric.*

Proof Let the surface S be scaled by a scalar $\alpha > 0$, such that

$$\tilde{S}(u, v) = \alpha S(u, v). \tag{8}$$

In what follows, we omit the surface parameterization u, v for brevity, and denote the a quantity y computed for the scaled surface by $\tilde{y}$. The first and second fundamental forms are scaled by α^2 and α respectively,

$$\begin{aligned} \tilde{g}_{ij} &= \langle \alpha S_i, \alpha S_j \rangle = \alpha^2 \langle S_i, S_j \rangle = \alpha^2 g_{ij}, \\ \tilde{b}_{ij} &= \langle \alpha S_{ij}, N \rangle = \alpha \langle S_{ij}, N \rangle = \alpha b_{ij}, \end{aligned} \tag{9}$$

which yields

$$\begin{aligned} \det(\tilde{g}) &= \alpha^4 \det(g) \\ \det(\tilde{b}) &= \alpha^2 \det(b). \end{aligned} \tag{10}$$

Since the Gaussian curvature is the ratio between the determinants of the second and first fundamental forms, we readily have that

$$\tilde{K} \equiv \frac{\det(\tilde{b})}{\det(\tilde{g})} = \frac{\alpha^2 \det(b)}{\alpha^4 \det(g)} = \frac{1}{\alpha^2} K, \tag{11}$$

from which we conclude that multiplying the Euclidean metric by the magnitude of its Gaussian curvature indeed provides a scale invariant metric. That is,

$$|\tilde{K}|\tilde{g}_{ij} = \left| \frac{1}{\alpha^2} K \right| \alpha^2 g_{ij} = |K| g_{ij}. \tag{12}$$

□

Theorem 2 *Let $r_{ij} = \det(S_1, S_2, S_{ij})$, and $q_{ij} = |r|^{-\frac{1}{4}} r_{ij}$, then, q_{ij} is an equi-affine invariant quadratic form.*

For proof see [55].

Corollary 1 *Let $Q = (q_{ij}) = \mathbf{U}\mathbf{\Gamma}\mathbf{U}^{\mathrm{T}}$ and $\mathbf{\Gamma} = \begin{pmatrix} \gamma_1 & 0 \\ 0 & \gamma_2 \end{pmatrix}$ then,*

$$\hat{Q} = \begin{cases} \mathbf{U} \begin{pmatrix} |\gamma_1| & 0 \\ 0 & |\gamma_2| \end{pmatrix} \mathbf{U}^{\mathrm{T}} & \text{if } \mathit{sign}(\gamma_1)\mathit{sign}(\gamma_2) > 0 \\ 0 & \text{if } \mathit{sign}(\gamma_1)\mathit{sign}(\gamma_2) \leq 0, \end{cases}$$

is an equi-affine invariant pseudo-metric.

Proof According to [55], the tensor Q is re-parametrization equi-affine invariant form for all elliptic points. For all elliptic points with $\gamma_1, \gamma_2 > 0$, we have the local metric structure $\hat{Q} = Q$. For all elliptic points with $\gamma_1, \gamma_2 < 0$, we use our freedom of surface orientation to obtain positive distances. In other words, by virtually changing the surface orientation we obtain a re-parametrization invariant metric structure with two positive eigenvalues, $\hat{Q} = \mathbf{U} \begin{pmatrix} |\gamma_1| & 0 \\ 0 & |\gamma_2| \end{pmatrix} \mathbf{U}^{\mathrm{T}}$. For all hyperbolic, and parabolic points we have a trivial invariant $\hat{Q} = 0$, that altogether construct the equi-affine invariant pseudo-metric. □

Using Brioschi formula [28] we can evaluate the Gaussian curvature directly from the metric and its first and second derivatives. Specifically, given the metric tensor q_{ij}, we have

$$K^q \equiv \frac{\beta - \gamma}{\det^2(q)}, \tag{13}$$

where

$$\begin{aligned}\beta &= \\ &\det\begin{pmatrix} -\frac{1}{2}q_{11,vv}+q_{12,vu}-\frac{1}{2}q_{22,uu} & \frac{1}{2}q_{11,u} & q_{12,u}-\frac{1}{2}q_{11,v} \\ q_{12,v}-\frac{1}{2}q_{22,u} & q_{11} & q_{12} \\ \frac{1}{2}q_{22,v} & q_{12} & q_{22} \end{pmatrix} \\ \gamma &= \det\begin{pmatrix} 0 & \frac{1}{2}q_{11,v} & \frac{1}{2}q_{22,u} \\ \frac{1}{2}q_{11,v} & q_{11} & q_{12} \\ \frac{1}{2}q_{22,u} & q_{12} & q_{22} \end{pmatrix},\end{aligned} \tag{14}$$

here $q_{ij,u}$ denotes the derivation of q_{ij} with respect to u, and in a similar manner $q_{ij,uv}$ is the second derivative w.r.t. u and v. Same notations follow for $q_{ij,v}$, $q_{ij,vv}$, and $q_{ij,uu}$.

Corollary 2 *Let q be the equi-affine metric. Then, K^q is an equi-affine invariant curvature.*

Proof From Brioschi's formula we have that the curvature can be evaluated directly from the metric and its derivatives. Hence, as by Corollary 1 the metric is equi-affine invariant, it follows that so does the equi-affine Gaussian curvature. □

Corollary 3 *Let K^q be the equi-affine invariant Gaussian curvature, then the metric defined by $h_{ij} = |K^q|\, q_{ij}$ is scale invariant.*

Proof Scaling the surface S by α, the corresponding equi-affine invariant components are

$$\begin{aligned}\tilde{r}_{ij} &= \det(\alpha S_1, \alpha S_2, \alpha S_{ij}) = \alpha^3 r_{ij} \\ \tilde{r}_{ij,u} &= \alpha^3 r_{ij,u} \\ \tilde{r}_{ij,uv} &= \alpha^3 r_{ij,uv} \\ \det(\tilde{r}) &= \alpha^6 \det(r),\end{aligned} \tag{15}$$

that leads to

$$\tilde{q}_{ij} = \frac{\tilde{r}_{ij}}{(\det(\tilde{r}))^{\frac{1}{4}}} = \frac{\alpha^3 r_{ij}}{(\alpha^6 \det(r))^{\frac{1}{4}}} = \alpha^{\frac{3}{2}} q_{ij}, \tag{16}$$

that yields $\det(\tilde{q}) = \left(\alpha^{\frac{3}{2}}\right)^2 \det(q) = \alpha^3 \det(q)$. Denote the equi-affine Gaussian curvature of the scaled surface $\tilde{S} = \alpha S$ by $\tilde{K}^q$. We have that

$$\begin{aligned}\tilde{\beta} &= \left(\alpha^{\frac{3}{2}}\right)^3 \beta, \\ \tilde{\gamma} &= \left(\alpha^{\frac{3}{2}}\right)^3 \gamma,\end{aligned}$$

$$\tilde{K}^q = \frac{\tilde{\beta}-\tilde{\gamma}}{\det^2(\tilde{q})} = \frac{\left(\alpha^{\frac{3}{2}}\right)^3(\beta-\gamma)}{(\alpha^3)^2 \det^2(q)} = \alpha^{-\frac{3}{2}} K^q. \tag{17}$$

It immediately follows that

$$|\tilde{K}^q|\tilde{q}_{ij} = |\tilde{K}^q|\alpha^{\frac{3}{2}} q_{ij} = |\alpha^{-\frac{3}{2}} K^q|\alpha^{\frac{3}{2}} q_{ij} = |K^q| q_{ij} \tag{18}$$

which concludes the proof. □

Theorem 3 *h_{ij} is an affine invariant pseudo-metric.*

Proof Putting corollaries 1, 2 and 3 together, we obtain the main result of this paper; Namely, h_{ij} is equi-affine invariant as well as scale invariant and thus affine invariant. □

4 Implementation considerations

Given a triangulated surface we use the Gaussian curvature approximation proposed in [37] while operating on the equi-affine metric tensor. The Gaussian curvature for smooth surfaces can be defined using the Global Gauss-Bonnet Theorem, see [24]. Polthier and Schmies used this property to approximate the Gaussian curvature of triangulated surfaces in [46]. Given a vertex in a triangulated mesh that is shared by p triangles such that the angle of each triangle at that vertex is given by θ_i, where $i \in 1, ...p$. The Gaussian curvature K at that vertex can be approximated by

$$K \cong \frac{1}{\frac{1}{3}\sum_{i=1}^{p} \mathcal{A}_i}\left(2\pi - \sum_{i=1}^{p}\theta_i\right), \tag{19}$$

where $\mathcal{A}_i$ is the area of the i-th triangle, and θ_i is the corresponding angle of the i-th triangle touching the vertex for which K is being approximated.

The metric tensor translates angles, distances, and areas from the parametric plane to the surface. Let us justify some known relations, as we use them in our numerical construction of the affine metric.

Corollary 4 *Consider a triangle $ABC = \{S(u_0, v_0), S(u_0 + du, v_0), S(u_0, v_0 + dv)\}$, infinitesimally defined on the surface $S(u, v)$ with metric (q_{ij}), then,*

$$\cos\theta_A = \frac{q_{12}}{\sqrt{q_{11}q_{22}}}. \tag{20}$$

Proof Consider the above infinitesimal triangle ABC. For simplicity of notations let $du = dv = 1$. The length of the edges of the triangle would then be $l_c^2 = (1\,0)(q_{ij})(1\,0)^T = q_{11}$, $l_b^2 = q_{22}$, and $l_a^2 = (1\,1)(q_{ij})(1\,1)^T = q_{11} - 2q_{12} + q_{22}$. From the law of cosines we readily have that

$$\cos\theta_A = \frac{q_{11} + q_{22} - (q_{11} - 2q_{12} + q_{22})}{2\sqrt{q_{11}q_{22}}} = \frac{q_{12}}{\sqrt{q_{11}q_{22}}}.$$

□

Corollary 5 *The area of the above triangle can be expressed by the metric coefficients as $\mathcal{A}_{ABC} = \frac{1}{2}\sqrt{\det(q_{ij})}$.*

Proof From Corollary 4 we have that

$$\sin^2\theta_A = 1 - \left(\frac{q_{12}}{\sqrt{q_{11}q_{22}}}\right)^2 = \frac{q_{11}q_{22} - q_{12}^2}{q_{11}q_{22}}.$$

The area of the triangle is half the length of its base multiplied by its height,

$$\mathcal{A}_{ABC} = \frac{1}{2}\sqrt{q_{22}}\left(\sqrt{q_{11}}\sqrt{\frac{q_{11}q_{22} - q_{12}^2}{q_{11}q_{22}}}\right) = \frac{1}{2}\sqrt{\det(q_{ij})}.$$

□

Consider the surface S given by its three coordinate functions $x(u,v)$, $y(u,v)$ and $z(u,v)$, where, for example, $x : U \in \mathbb{R}^2 \rightarrow \mathbb{R}$, and

$$S(u,v) = \begin{pmatrix} x(u,v) \\ y(u,v) \\ z(u,v) \end{pmatrix}. \tag{21}$$

In order to evaluate the equi-affine metric the surface is first locally approximated by a quadratic form. For each triangle we approximate

$$S(u,v) = \begin{pmatrix} x(u,v) \\ y(u,v) \\ z(u,v) \end{pmatrix} \approx C \begin{pmatrix} 1 \\ u \\ v \\ uv \\ u^2 \\ v^2 \end{pmatrix}. \tag{22}$$

where the matrix $C_{3\times 6}$ contains 18 parameters. The local coefficients matrix C is evaluated from six surface points (vertices). Three vertices belong to the triangle for which the metric is evaluated, and three to its nearest neighboring triangles.

The equi-affine metric coefficients for each triangle are then evaluated from our local quadratic approximation of $S(u,v)$ and its corresponding derivatives. Finally, the Gaussian curvature with respect to the equi-affine metric is approximated for each vertex from the local area and angle distortions as defined by the metric, see Eq. (19). In order to construct the full-affine invariant metric we need to scale the equi-affine metric by the equi-affine Gaussian curvature. To that end, the curvature is linearly interpolated, from its values at the vertices, at the center of each triangle.

Finally, following [48], we use the finite elements method (FEM) presented in [25] to compute the spectral decomposition of the affine invariant Laplace-Beltrami operator constructed from the metric provided by Eq. (7). The decomposition based on an affine invariant pseudo-metric provides invariant eigenvectors and corresponding invariant eigenvalues.

The equi-affine metric is well defined only at elliptic points [55], that is, points with positive Euclidean Gaussian curvature. At parabolic and hyperbolic points the equi-affine metric trivially degenerates to zero, while at elliptic points the local surface orientation is defined so as to provide positive distances. In order, to numerically handle non-elliptic surface points we assigned a small $\epsilon\mathcal{I}$ to be the metric matrix. The $O(\epsilon)$ error introduced to geodesic distances measured with such a regularization is bounded by $\epsilon\mathcal{D}$, where $\mathcal{D}$ is the diameter of the surface. As many interesting shapes are dominated by elliptic points, the error is often smaller than the above upper bound.

5 Metric invariant diffusion geometry

Diffusion Geometry introduced in [22,21], deals with geometric analysis of metric spaces where usual distances are replaced by integral difference between heat kernels. The *heat equation*

$$\left(\frac{\partial}{\partial t} + \Delta_h\right) f(x,t) = 0, \tag{23}$$

describes the propagation of heat, where $f(x,t)$ is the heat distribution at a point x in time t. Initial conditions are given as $f(x,0)$, and Δ_h is the Laplace Beltrami operator with respect to the metric h. The fundamental solution of (23) is called a *heat kernel*, and using spectral decomposition it can be written as

$$k_t(x,x') = \sum_{i\geq 0} e^{-\lambda_i t}\phi_i(x)\phi_i(x'), \tag{24}$$

where ϕ_i and λ_i are the corresponding eigenfunctions and eigenvalues of the Laplace-Beltrami operator satisfying

$$\Delta_h\phi_i = \lambda_i\phi_i. \tag{25}$$

As the Laplace-Beltrami operator is an *intrinsic* geometric quantity, it can be expressed in terms of a metric h of the surface $\mathcal{S}$.

The value of the heat kernel $k_t(x,x')$ can be interpreted as the transition probability density of a random walk of length t from point x to point x'. The length or time t defines a family of diffusion distances

$$\begin{aligned} d_t^2(x,x') &= \int \left(k_t(x,\cdot) - k_t(x',\cdot)\right)^2 da \\ &= \sum_{i>0} e^{-2\lambda_i t}(\phi_i(x) - \phi_i(x'))^2, \end{aligned} \tag{26}$$

between any two surface points x and x'. Special attention was given to the diagonal of the kernel $k_t(x,x)$, that was proposed as robust local descriptor, and referred to as the *heat kernel signatures* (HKS), by Sun *et al.* in [56].

6 Experimental results

The first experiment presents eigenfunctions of the Laplace Beltrami operator defined by various metrics and different deformations. In Figure 2 we present the 9'th eigenfunction textured mapped on the surface using a Euclidean metric, scale invariant, equi-affine and the proposed affine invariant pseudo-metric. At each row a different deformation of the surface is presented. Local scaling was applied to the shapes at the second row, while surfaces on the third row underwent volume preserving stretching (equi-affine). The bottom row shows a full affine transformation that was applied to the surface (including local scaling). The accumulated histogram values of the corresponding 9'th eigenfunction are plotted at the top of each column. Blue is used for the original shape,

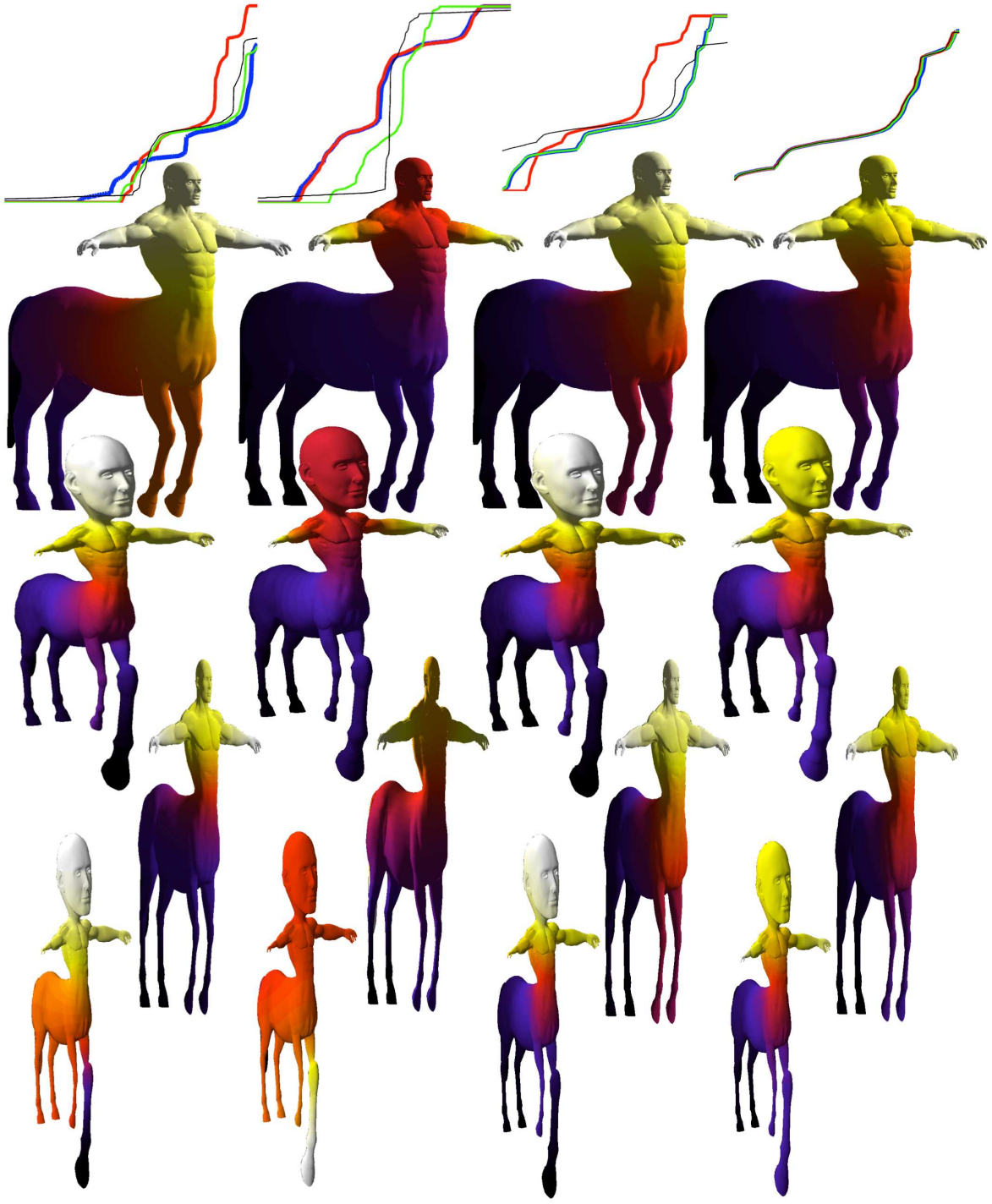

Fig. 2: The 9'th LBO eigenfunction textured mapped on the surface using four different metrics, from left to right: Euclidean, scale-invariant, equi-affine, and affine. Deformations from top to bottom: None, local scale, equi-affine, and affine. At the top, the accumulated (histogram) values of the eigenfunction are displayed. The blue curve depicts the original shape, red the a locally scaled one, green the equi-affine and black the affine transformation.

red for the locally scaled one, green for the equi-affine transformed one, and black for the affine transformed version.

In the second experiment, shown in Figure 3, we evaluate the Heat Kernel Signatures of a surface subject to an affine transformations using the Euclidean metric and the affine pseudo-metric. We plot the signatures using log-log axes for three different corresponding points on the surfaces.

The third experiment, Figure 4 shows diffusion distances measured from the nose of a cat after anisotropic scaling and stretching as well as an almost isomeric pose transformation.

Next, we compute the Voronoi diagrams for ten points selected by the farthest point sampling strategy, as seen in Figures 5 and 1. Distances are measured with the global scale invariant commute time distances [47], and diffusion distances receptively, using a Euclidean and the proposed affine metrics. Again, the affine metric is proven to be invariant to affine transformations as expected.

In the next experiment we used the affine metric for finding the correspondence between two shapes. We used the GMDS framework [8] with diffusion distances using the same initialization for both experiments. Figure 6 displays the Voronoi cells of matching surface segments.

Finally, we evaluated the proposed metric on the SHREC 2010 dataset [7] using the shapeGoogle framework [42], while introducing four new deformations; equi-affine, isometry and equi-affine, affine, and a combination of isometry and affine. Table 1 shows that the new affine metric discriminative power is as good as the Euclidean one, performs well on scaling as the scale invariant metric, and similar to the equi-affine one for handling volume preserving affine transformations. Moreover, the new metric is the only one capable of dealing with the full affine deformations. Note that shapes which were considered to be locally scaled in that database, were in fact treated with an offset operation (morphological erosion) rather than scaling. This explains part of the performance degradation in the local scale examples.

Performance was evaluated using precision/recall characteristics. *Precision* $\mathrm{P}(r)$ is defined as the percentage of relevant shapes in the first r top-ranked retrieved shapes. *Mean average precision* (mAP) is defined as $\mathrm{mAP} = \sum_r \mathrm{P}(r) \cdot \mathrm{rel}(r)$, where $\mathrm{rel}(r)$ the relevance of a given rank, was used as a single measure of performance. Intuitively, mAP is interpreted as the area below the precision-recall curve. Ideal retrieval (mAP=100%) is achieved when all queries provide the correct answer as first match. Performance results are summarized by the transformation class and strength.

7 Conclusions

A new affine invariant pseudo-metric for surfaces was introduced. Assuming the limbs of an articulated objects are connected with non-elliptic regions, the proposed differential structure allows us to cope with per-limb stretching and scaling of the surface. We demonstrated the proposed geometry by incorporating it with known shape analysis tools that were evaluated by computing the correspondence, matching, and retrieval of synthetic surfaces. The power to deal with a richer set of transformations when analyzing shapes has already proven to be useful in the analysis of textured shapes as shown in [32]. We hope that the proposed affine geometry could be found useful in the future for shape processing and analysis applicants.

8 Acknowledgement

We thank the editor and the reviewers for their valuable comments that helped us improve the presentation and writeup of the paper. This research was supported by the Office of Naval Research (ONR) award number N00014-12-1-0517 and by Israel Science Foundation (ISF) grant number 1031/12.

References

1. Y. Aflalo, R. Kimmel, and D. Raviv. Scale invariant geometry for nonrigid shapes. *SIAM J. on Imaging Sciences*, 6(3):1579–1597, 2013. 2, 3
2. L. Alvarez, F. Guichard, P.-L. Lions, and J.-M. Morel. Axioms and fundamental equations of image processing. *Archive for Rational Mechanics and Analysis*, 123(3):199–257, 1993. 1
3. M. Andrade and T. Lewiner. Affine-invariant curvature estimators for implicit surfaces. *Computer Aided Geometric Design*, 29(2):162–173, 2012. 2
4. M. F. Beg, M. I. Miller, Trouvé A., and L. Younges. Computing large deformation metric mappings via geodesic flows of diffeomorphisms. *International Journal of Computer Vision (IJCV)*, 61(2):139–157, 2005. 1
5. P. Bérard, G. Besson, and S. Gallot. Embedding Riemannian manifolds by their heat kernel. *Geometric and Functional Analysis*, 4(4):373–398, 1994. 1
6. W. Blaschke. *Vorlesungen uber Differentialgeometrie und geometrische Grundlagen von Einsteins Relativitatstheorie*, volume 2. Springer, 1923. 2
7. A. M. Bronstein, M. M. Bronstein, U. Castellani, B. Falcidieno, A. Fusiello, A. Godil, L. J. Guibas, I. Kokkinos, Z. Lian, M. Ovsjanikov, G. Patané, M. Spagnuolo, and R. Toldo. SHREC 2010: robust large-scale shape retrieval benchmark. In *Proc. Workshop on 3D Object Retrieval (3DOR)*, 2010. 7
8. A. M. Bronstein, M. M. Bronstein, and R. Kimmel. Efficient computation of isometry-invariant distances between surfaces. *SIAM journal on Scientific Computing*, 28(5):1812–1836, 2006. 1, 7, 9
9. A. M. Bronstein, M. M. Bronstein, R. Kimmel, M. Mahmoudi, and G. Sapiro. A Gromov-Hausdorff framework with diffusion geometry for topologically-robust non-rigid shape matching. *International Journal of Computer Vision (IJCV)*, 89(2-3):266–286, 2010. 1
10. M. M. Bronstein and I. Kokkinos. Scale-invariant heat kernel signatures for non-rigid shape recognition. In *Proc. Computer Vision and Pattern Recognition (CVPR)*, 2010. 2
11. A. Brook, A.M. Bruckstein, and R. Kimmel. On similarity-invariant fairness measures. In *Scale-Space*, LNCS 3459, pages 456–467, Hofgeismar, Germany, 7-9 April 2005. Springer-Verlag. 1

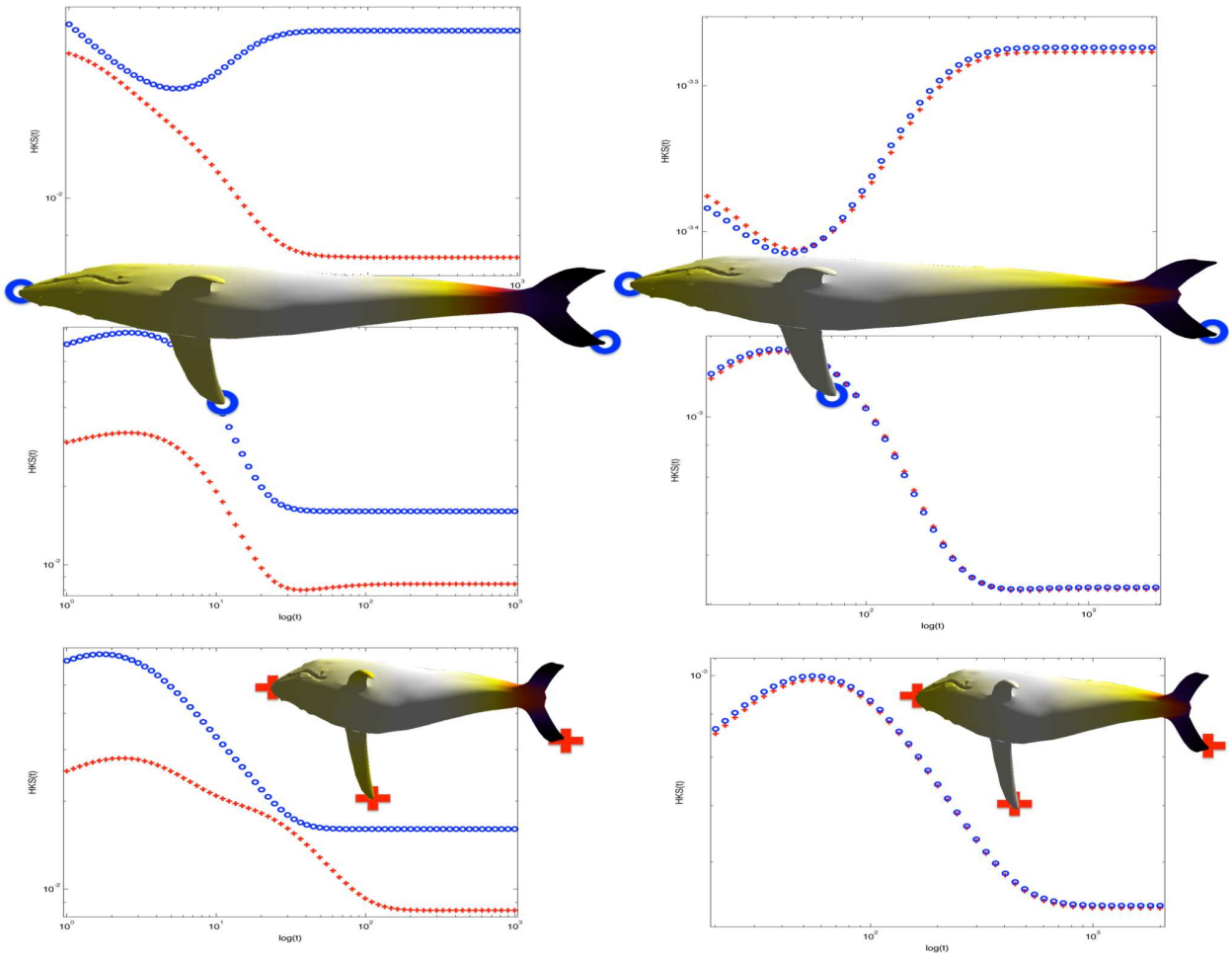

Fig. 3: Affine heat kernel signatures for the regular metric (left), and the invariant version (right). The blue circles represent the signatures for three points on the original surface, while the red plus signs are computed for the deformed version. Using log-log axes, we plot the scaled-HKS as a function of t.

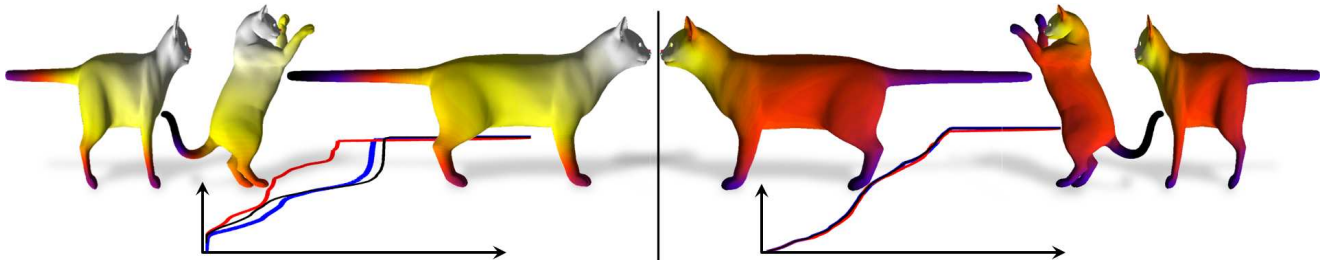

Fig. 4: Diffusion distances - Euclidean (left) and affine (right) - is measured from the nose of the cat after non-uniform scaling and stretching. The accumulated (histogram) distances (at the bottom) are color-coded as in Figure 2.

12. A. M. Bruckstein, R. J. Holt, A. N. Netravali, and T. J. Richardson. Invariant signatures for planar shape recognition under partial occlusion. *Computer Vision, Graphics, and Image Processing: Image Understanding*, 58:49–65, 1993. 1

13. A. M. Bruckstein, N. Katzir, M. Lindenbaum, and M. Porat. Similarity-invariant signatures for partially occluded planar shapes. *International Journal of Computer Vision*, 7(3):271–285, 1992. 1

14. A. M. Bruckstein and A. N. Netravali. On differential invariants of planar curves and recognizing partially occluded planar shapes. *Annals of Mathematics and Artificial Intelligence (AMAI)*, 13(3-4):227–250, 1995. 1

15. A. M. Bruckstein, E. Rivlin, and I. Weiss. Scale-space local invariants. *Image and Vision Computing*, 15(5):335–344, 1997. 1

16. A.M. Bruckstein and D. Shaked. Skew symmetry detection via invariant signatures. *Pattern Recognition*, 31(2):181–192, 1998. 1

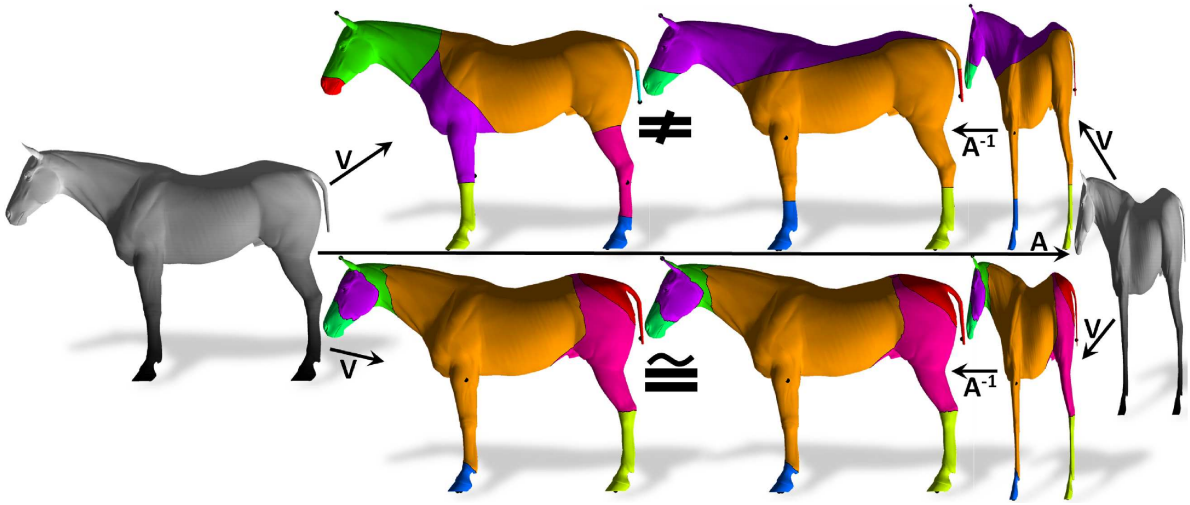

Fig. 5: Voronoi diagrams using ten points selected by the farthest point sampling strategy. The commute time distances were evaluated using the Euclidean metric (top) and the proposed affine one (bottom).

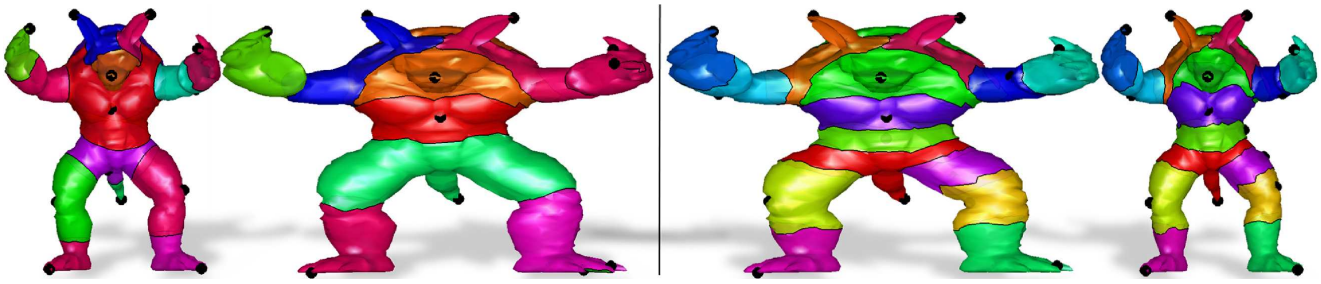

Fig. 6: Matching two shapes using the GMDS [8] framework with diffusion distances. The affine (right) metric finds the proper correspondence as expected unlike the Euclidean one (left) which is sensitive to non-uniform stretching. Corresponding surface segments share the same color.

17. E. Calabi, P.J. Olver, C. Shakiban, A. Tannenbaum, and S. Haker. Differential and numerically invariant signature curves applied to object recognition. *International Journal of Computer Vision*, 26:107–135, 1998. 1
18. S. Carlsson, R. Mohr, T. Moons, L. Morin, C. A. Rothwell, M. Van Diest, L. Van Gool, F. Veillon, and A. Zisserman. Semi-local projective invariants for the recognition of smooth plane curves. *International Journal of Computer Vision*, 19(3):211–236, 1996. 1
19. F. Chazal, D. Cohen-Steiner, L.J. Guibas, F. Mémoli, and S. Oudot. Gromov-Hausdorff stable signatures for shapes using persistence. *Computer Graphics Forum*, 28(5):1393–1403, July 2009. 1
20. T. Cohignac, C. Lopez, and J.M. Morel. Integral and local affine invariant parameter and application to shape recognition. In *Proceedings of the 12th IAPR International Conference on Pattern Recognition (ICPR)*, volume 1, pages 164–168, October 1994. 1
21. R. R. Coifman and S. Lafon. Diffusion maps. *Applied and Computational Harmonic Analysis*, 21:5–30, July 2006. 5
22. R. R. Coifman, S. Lafon, A. B. Lee, M. Maggioni, B. Nadler, F. Warner, and S. W. Zucker. Geometric diffusions as a tool for harmonic analysis and structure definition of data: Diffusion maps. *PNAS*, 102(21):7426–7431, 2005. 1, 5
23. R.H. Davies, C.J. Twining, T.F. Cootes, J.C. Waterton, and C.J. Taylor. A minimum description length approach to a minimum description length approach to statistical shape modeling. *IEEE Trans. Medical Imaging*, 21(5), 2002. 1
24. M. P. do Carmo. *Differential geometry of curves and surfaces*. Prentice-Hall, 1976. 4
25. G. Dziuk. Finite elements for the Beltrami operator on arbitrary surfaces. In *Partial differential equations and calculus of variations*, pages 142–155. 1988. 5
26. A. Elad and R. Kimmel. Bending invariant representations for surfaces. In *Proc. Computer Vision and Pattern Recognition (CVPR)*, pages 168–174, 2001. 1
27. P. T. Fletcher, S. Joshi, , C. Lu, and S. Pizer. Gaussian distributions on Lie groups and their application to statistical shape analysis. In *Proc. Information Processing in Medical Imaging (IPMI)*, pages 450–462, 2003. 1
28. A. Gray, E. Abbena, and S. Salamon. *Modern Differential Geometry of Curves and Surfaces with Mathematica*. 3rd edition, 2006. 3
29. A.B. Hamza and H. Krim. Geodesic matching of triangulated surfaces. *IEEE Transactions on Image Processing*, 15(8):2249–2258, 2006. 1
30. H. Huang, L. Shen, R. Zhang, F. Makedon, B. Hettleman, and J. D. Pearlman. Surface alignment of 3D spherical harmonic models: Application to cardiac MRI analysis. In *Proc. Medical Image Computing and Computer Assisted Intervention (MICCAI)*, 2005. 1
31. R. Kimmel. Affine differential signatures for gray level images of planar shapes. In *Proceedings of the 13th International Conference on Pattern Recognition*, pages 45–49, vol. 1, Vienna, Austria, 25-30 August 1996. IEEE. 1
32. A. Kovnatsky, M. M. Bronstein, D. Raviv, A. M. Bronstein, and R. Kimmel. Affine-invariant photometric heat kernel signatures.

Euclidean invariant metric

Transformation	Strength 1	≤2	≤3	≤4	≤5
Isometry	100.00	100.00	100.00	100.00	100.00
Micro holes	100.00	100.00	100.00	100.00	100.00
Noise	100.00	100.00	100.00	98.72	98.97
Shot noise	100.00	100.00	98.72	97.60	97.05
Scale	28.87	56.74	61.42	53.75	47.77
Local scale	100.00	100.00	98.72	91.79	87.40
Equi-Affine	100.00	98.08	92.52	87.72	83.05
Iso+Equi-Affine	100.00	97.12	92.95	85.32	79.99
Affine	88.46	77.79	70.81	65.21	61.21
Isometry+Affine	88.46	77.82	73.76	68.35	64.60

Scale invariant metric

Strength 1	≤2	≤3	≤4	≤5
100.00	100.00	100.00	100.00	100.00
100.00	92.12	84.66	78.90	74.96
100.00	95.00	92.42	87.49	81.62
100.00	100.00	97.01	94.94	92.21
100.00	100.00	100.00	100.00	100.00
100.00	97.44	94.87	90.21	82.98
81.03	72.35	65.82	61.55	59.86
81.03	74.13	63.93	61.17	62.30
100.00	90.87	87.36	84.64	81.99
100.00	93.75	89.64	84.33	83.11

Equi-affine invariant pseudo-metric

Transformation	Strength 1	≤2	≤3	≤4	≤5
Isometry	100.00	100.00	100.00	100.00	100.00
Micro holes	100.00	100.00	100.00	100.00	100.00
Noise	100.00	100.00	91.88	83.72	75.62
Shot noise	100.00	100.00	100.00	97.12	92.31
Scale	29.82	50.81	48.34	43.16	39.89
Local scale	100.00	100.00	95.51	87.81	81.08
Equi-Affine	100.00	100.00	100.00	100.00	100.00
Iso+Equi-Affine	100.00	100.00	100.00	100.00	100.00
Affine	75.90	60.35	52.54	47.82	43.86
Isometry+Affine	75.46	59.59	52.08	47.39	44.34

Affine invariant pseudo-metric

Strength 1	≤2	≤3	≤4	≤5
100.00	100.00	98.72	99.04	99.23
100.00	100.00	98.08	97.02	95.53
100.00	95.51	94.02	94.55	94.87
100.00	100.00	100.00	99.04	97.69
94.87	97.44	98.29	95.03	92.40
100.00	100.00	98.29	96.47	92.07
100.00	100.00	96.79	96.63	96.08
100.00	98.08	93.80	94.39	94.36
96.15	95.51	95.73	95.83	96.67
96.15	98.08	97.44	98.08	98.46

Table 1: Performance of different metrics with shapeGoogle framework(mAP in %).

In *Proc. Eurographics workshop on 3D object retrieval (3DOR)*, 2012. 7

33. H. Ling and D.W. Jacobs. Using the inner-distance for classification of articulated shapes. In *Proc. Computer Vision and Pattern Recognition (CVPR)*, volume 2, pages 719–726, San Diego, USA, 20-26 June 2005. 1
34. Y. Lipman and T. Funkhouser. Möbius voting for surface correspondence. In *Proc. ACM Transactions on Graphics (SIGGRAPH)*, volume 28, 2009. 1
35. D. Lowe. Distinctive image features from scale-invariant keypoint. *International Journal of Computer Vision (IJCV)*, 60(2):91–110, 2004. 1
36. F. Mémoli and G. Sapiro. A theoretical and computational framework for isometry invariant recognition of point cloud data. *Foundations of Computational Mathematics*, 5(3):313–347, 2005. 1
37. M. Meyer, M. Desbrun, P. Schroder, and A. H. Barr. Discrete differential-geometry operators for triangulated 2-manifolds. *Visualization and Mathematics III*, pages 35–57, 2003. 4
38. T. Moons, E. Pauwels, L.J. Van Gool, and A. Oosterlinck. Foundations of semi-differential invariants. *International Journal of Computer Vision (IJCV)*, 14(1):25–48, 1995. 1
39. J. M. Morel and G. Yu. ASIFT: A new framework for fully affine invariant image comparison. *SIAM Journal on Imaging Sciences*, 2:438–469, 2009. 1
40. P. J. Olver. Joint invariant signatures. *Foundations of Computational Mathematics*, 1:3–67, 1999. 1
41. P.J. Olver. A survey of moving frames. In H. Li, P.J. Olver, and G. Sommer, editors, *Computer Algebra and Geometric Algebra with Applications*, LNCS 3519, pages 105–138, New York, 2005. Springer-Verlag. 1
42. M. Ovsjanikov, A. M. Bronstein, M. M. Bronstein, and L. J. Guibas. Shape Google: a computer vision approach to invariant shape retrieval. In *Proc. Non-Rigid Shape Analysis and Deformable Image Alignment (NORDIA)*, 2009. 1, 7
43. M. Ovsjanikov, Q. Mérigot, F. Mémoli, and L. J. Guibas. One point isometric matching with the heat kernel. In *Proc. Symposium on Geometry Processing (SGP)*, volume 29, pages 1555–1564, 2010. 1
44. E. Pauwels, T. Moons, L.J. Van Gool, P. Kempenaers, and A. Oosterlinck. Recognition of planar shapes under affine distortion. *International Journal of Computer Vision (IJCV)*, 14(1):49–65, 1995. 1
45. X. Pennec. Intrinsic statistics on Riemannian manifolds: Basic tools for geometric measurements. *Journal of Mathematical Imaging and Vision (JMIV)*, 25(1):127–154, 2006. 1
46. K. Polthier and M. Schmies. Straightest geodesics on polyhedral surfaces. *Mathematical Visualization*, 1998. 4
47. H. Qiu and E.R. Hancock. Clustering and embedding using commute times. *IEEE Transactions on Pattern Analysis and Machine Intelligence*, 29(11):1873–1890, November 2007. 7
48. D. Raviv, A. M. Bronstein, M. M. Bronstein, R. Kimmel, and N. Sochen. Affine-invariant diffusion geometry of deformable 3D shapes. In *Proc. Computer Vision and Pattern Recognition (CVPR)*, 2011. 2, 3, 5
49. D. Raviv, A. M. Bronstein, M. M. Bronstein, R. Kimmel, and N. Sochen. Affine-invariant geodesic geometry of deformable 3D shapes. *Computers & Graphics*, 35(3):692–697, 2011. 2
50. D. Raviv, A. M. Bronstein, M. M. Bronstein, D. Waisman, N. Sochen, and R. Kimmel. Equi-affine invariant geometry for shape analysis. *Journal of Mathematical Imaging and Vision (JMIV)*, 2013. 3
51. M. Reuter, H.D. Rosas, and B. Fischl. Highly accurate inverse consistent registration: A robust approach. *Neuroimage*, 53(4):1181–1196, 2010. 1

52. J. Rugis and R. Klette. A scale invariant surface curvature estimator. In *Advances in Image and Video Technology, First Pacific Rim Symposium (PSIVT)*, volume 4319, pages 138–147, 2006. 2
53. R. Rustamov. Laplace-Beltrami eigenfunctions for deformation invariant shape representation. In *Proc. Symposium on Geometry Processing (SGP)*, pages 225–233, 2007. 1
54. G. Sapiro. *Affine Invariant Shape Evolutions*. PhD thesis, Technion - IIT, 1993. 1
55. B. Su. *Affine differential geometry*. Beijing, China: Science Press, 1983. 2, 3, 5
56. J. Sun, M. Ovsjanikov, and L. J. Guibas. A concise and provably informative multi-scale signature based on heat diffusion. In *Proc. Symposium on Geometry Processing (SGP)*, 2009. 1, 5
57. L. Van Gool, M. Brill, E. Barrett, T. Moons, and E.J. Pauwels. Semi-differential invariants for nonplanar curves. In J. Mundy and A. Zisserman, editors, *Geometric Invariance in Computer Vision*, pages Chapter 11: 293–309, Massachusetts / London, Englad, 1992. MIT Press: Cambridge. 1
58. L. Van Gool, T. Moons, E.J. Pauwels, and A. Oosterlinck. Semi-differential invariants. In J. Mundy and A. Zisserman, editors, *Geometric Invariance in Computer Vision*, pages Chapter 8: 157–192, Massachusetts / London, England, 1992. MIT Press: Cambridge. 1
59. Y. Wang, M. Gupta, S. Zhang, S. Wang, X. Gu, D. Samaras, and P. Huang. High resolution tracking of non-rigid motion of densely sampled 3D data using harmonic maps. *International Journal of Computer Vision (IJCV)*, 76(3):283–300, 2008. 1
60. I. Weiss. Projective invariants of shapes. Technical Report CAR-TR-339, University of Maryland - Center for Automation, January 1988. 1